

AFFDL-TM-78-66-FBT/FBE

**AIR FORCE FLIGHT DYNAMICS LABORATORY
DIRECTOR OF SCIENCE & TECHNOLOGY
AIR FORCE SYSTEMS COMMAND
WRIGHT-PATTERSON AIR FORCE BASE OHIO**



**AN EXPLORATORY STUDY OF DAMAGE ACCUMULATION
METHODS FOR PROPAGATING FATIGUE CRACKS**

**G.W. Trickle, R.A. Kleismit
H.D. Stalnaker, J.E. Grove
(FBT)**

**J.P. Gallagher
(FBE)**

Technical Memorandum AFFDL-TM-78-66-FBT/FBE

June 1978

**Reproduced From
Best Available Copy**

Approved for Public Release; Distribution Unlimited

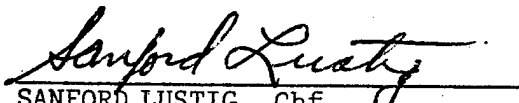
19990806 035


**RETURN TO: AEROSPACE STRUCTURES
INFORMATION AND ANALYSIS CENTER
AFFDL/FBR
WPAFB, OHIO 45433**

NOTICES

When Government drawings, specifications, or other data are used for any purpose other than in connection with a definitely related Government procurement operation, the United States Government thereby incurs no responsibility nor any obligation whatsoever; and the fact that the government may have formulated, furnished, or in any way supplied the said drawings, specifications, or other data, is not to be regarded by implication or otherwise as in any manner licensing the holder or any other person or corporation, or conveying any rights or permission to manufacture, use or sell any patented invention that may in any way be related thereto.

This technical report has been reviewed and is approved for publication.


SANFORD LUSTIG, Chf
Structures Test Branch


ROBERT M. BADER, Chf
Structural Integrity Branch

This report has been reviewed and cleared for open publication and/or public release by the appropriate Office of Information (OI) in accordance with AFR 190-17 and DODD 5230.9. There is no objection to unlimited distribution of this report to the public at large or by DDC to the National Technical Information Service (NTIS).

Copies of this report should not be returned unless return is required by security considerations, contractual obligations, or notice on a specific document.

RETURN TO: AEROSPACE STRUCTURES
INFORMATION AND ANALYSIS CENTER
AFFDL/FBR
WPAFB, OHIO 45433

ABSTRACT

This report presents three methods that predict damage accumulation and crack initiation lives for notched laboratory specimens that were subjected to stepwise increasing load. Constant load amplitude and monotonic tensile tests provide the necessary baseline data for establishing the relationship between cyclic loads applied and the damage accumulation process.

FOREWARD

This program was conducted by Glen W. Trickle, project engineer, Air Force Flight Dynamics Laboratory (AFFDL), Wright-Patterson Air Force Base, Ohio 45433. The work was conducted under in-house project number, 2307φ101, in the Fatigue and Fracture subfacility in Building 65 of the Air Force Flight Dynamics Laboratory. In addition, the following individuals participated in the development and support of the test program: Richard Kleismit, James E. Grove, and Harold D. Stalnaker. Dr. J. P. Gallagher of AFFDL/FBE acted as program manager. This report covers the work accomplished over a time period of August 1 to December 31, 1976.

This page left blank.

TABLE OF CONTENTS

| <u>SECTION</u> | | <u>PAGE</u> |
|----------------------|---|-------------|
| I | INTRODUCTION | 1 |
| II | EXPERIMENTAL METHODS AND PROCEDURES | 3 |
| III | NON-CONSTANT AMPLITUDE TESTING | 15 |
| IV | CONCLUSIONS | 27 |
| V | REFERENCES | 28 |
| | | 29 |
| APPENDIX A | | |

LIST OF FIGURES

| <u>FIGURE</u> | | <u>PAGE</u> |
|---------------|---|-------------|
| 1 | Test Geometry For Initial Damage Accumulation Study. | 7 |
| 2 | Monotonic Test Data. | 7 |
| 3 | Programmed Constant Amplitude Loading For Test Number 10. | 8 |
| 4 | Constant Amplitude Test Data For Test Number 10. | 8 |
| 5 | Plastic Crosshead Displacement Accumulation As A Function Of Constant Amplitude Cycles For Test 10. | 9 |
| 6 | Plastic Crosshead Displacement Versus Cycles To Initiate A Crack. Based On Average Plastic Crosshead Displacement Values. | 13 |
| 7 | Neuber Parameter Versus Cycles To Initiate A Crack Based On Average Cyclic Values Of The Neuber Parameter. | 13 |
| 8 | Programmed Stepwise Increasing Amplitude Loading For Test Number 12. | 19 |
| 9 | Stepwise Increasing Amplitude Test Data For Test Number 12. | 19 |
| 10 | Plastic Crosshead Displacement As A Function Of Cycles For Test Number 12. | 20 |
| 11 | Damage Accumulation As A Function of Stress Level For Test Number 12. | 21 |
| 12 | Test Specimen Gross Stress As A Function of Accumulated Plastic Crosshead Displacement. | 21 |
| A-1 | Plastic Crosshead Displacement VS. Cycles To Failure For Slot Geometry. | 33 |
| A-2 | Neuber Parameter VS. Cycles To Failure For Slot Geometry. | 33 |

LIST OF TABLES

| <u>TABLE</u> | <u>PAGE</u> |
|---|-------------|
| I DATA FROM MONOTONIC TESTS | 5 |
| II DATA FROM CONSTANT AMPLITUDE TESTS | 6 |
| III DAMAGE SUMMATIONS BASED ON AVERAGE PER CYCLE MEASUREMENTS ($\Sigma D > 1$, CONSERVATIVE) | 14 |
| IV RESULTS FOR INITIAL STEPWISE INCREASING LOAD TESTS | 16 |
| V DAMAGE METHODS COMPARED FOR INITIAL STEPWISE INCREASING LOAD TESTS | 16 |
| VI VERIFICATION LIFE ESTIMATES (CYCLES TO FAILURE) BASED ON THE THREE DAMAGE METHODS | 18 |
| VII CONDITIONS FOR A NEW SET OF STEPWISE INCREASING FATIGUE LOAD TESTS | 23 |
| VIII LIFE ESTIMATES (CYCLES TO FAILURE) FOR A NEW SET OF STEPWISE INCREASING FATIGUE LOAD TESTS | 23 |
| IX FAILURE DATA FOR SECOND SET OF STEPWISE-INCREASING LOAD TESTS | 24 |
| X DAMAGE CALCULATIONS FOR STEP-WISE INCREASING LOAD TESTS DESCRIBED BY TABLE IX; BASED ON PLASTIC DISPLACEMENT TEST RESULTS | 24 |
| XI DAMAGE CALCULATIONS SUMMARIZED FOR ALL TESTS | 26 |

APPENDIX A

| <u>TABLE</u> | <u>PAGE</u> |
|---|-------------|
| A1 SUMMARY OF TEST DATA FOR SLOTTED TEST SPECIMENS | 31 |
| A2 DAMAGE CALCULATIONS SUMMARIZED FOR SLOTTED SPECIMENS | 32 |

SECTION I

INTRODUCTION

A number of investigators (1-4) have studied the stresses and strains in the vicinity of (quasi) stationary crack tips for the specific purpose of modeling the fatigue crack growth process. Each study suggested that a fatigue crack initiation-type damage relationship could be used in conjunction with uniaxial stress-strain properties to determine the rate at which fatigue cracks propagate. This report describes an experimental study that was initiated to demonstrate how the fatigue damage ahead of a growing crack tip might actually accumulate.

The basic hypothesis for the earlier studies was that the damage accumulation process (DAP) occurring in each material element located in the path of the propagating fatigue crack tip controls the rate of crack propagation. The damage accumulation calculations were made by assuming that the DAP can be described by the behavior experienced by an unnotched, unconstrained, fatigue coupon subjected to the analytically derived uniaxial loadings associated with the element location. In this report, notched fatigue coupons are subjected to constant stepwise increasing (with each cycle) sawtooth fatigue loading histories. The notch geometry was chosen in an attempt to experimentally stimulate the localized material-geometrical constraints that might be experienced in an element located in advance of a propagating crack tip. The constant stepwise increasing sawtooth histories were chosen to provide a first-order simulation of the type of loading experienced by an element located in the path of the advancing crack tip.

The objective of the investigation was to determine if the fatigue behavior of the notched coupons that were subjected to the stepwise increasing sawtooth loading could be described and predicted using fatigue crack initiation analysis methods. Since this was an exploratory effort, the baseline data for predicting cycles to crack initiation were established with notched coupons of the same design as that used in the stepwise increasing sawtooth tests. Correlation of fatigue lives observed for the stepwise increasing sawtooth loading histories were made with estimates established using damage relationships based on the constant amplitude fatigue and monotonic load test results. These damage accumulation relationships follow those suggested by uniaxial fatigue initiation damage studies (Ref. 5 provides a good background reference on these studies) and include:

1. A plastic displacement range ($\Delta\delta_{pl}$) vs life relationship.
2. A Neuber parameter, gross stress range ($\Delta\sigma_g$) multiplied by the plastic displacement range ($\Delta\delta_{pl}$), vs life relationship.
3. A scheme based on the ratio of the accumulated tensile plastic displacement range to the monotonic plastic displacement (δ_{pl}^{cr}) that causes onset of fracture.

SECTION II

EXPERIMENTAL METHODS AND PROCEDURES

MEASUREMENTS AND CONTROL

The initial set of tests designed to develop and subsequently verify the damage accumulation methods were performed on copper specimens of the type shown in Fig. 1. The mechanical properties of the copper, based on 0.500 inch (12.7 mm) diameter tensile specimens were found to be:

| | |
|------------------------------|------------|
| 0.2% offset yield strength | 32.9 ksi |
| Ultimate strength | 36.2 ksi |
| Modulus of elasticity | 16,000 ksi |
| Reduction in area at failure | 50.8% |

Testing in this program was performed using a 100 kip MTS servo-hydraulic test machine in which loads were measured and controlled using a four bridge Interface load cell in series with the specimen. An on-line PDP 11/40 computer was used to measure loads within an accuracy of 0.5% of the full scale load. Crosshead displacements were measured using an LVDT gage mounted on the loading cylinder. The LVDT device exhibited a linearity of 0.2% over a full scale range of 3.0 inches. A permanent record of the displacement and load data obtained during the tests was provided by an Electro-Instruments, Inc. XY recorder.

MONOTONIC TESTS

A set of tests was run to establish the constants used in the damage accumulation prediction equations. The first tests were monotonic tensile load tests in which specimens of the type shown in Fig. 1

were fractured. A sample load-displacement curve for one of these tests is shown in Fig. 2. Also shown in Fig. 2 is the measured ultimate-load displacement that occurred prior to instability. For the monotonic tests, failure is defined to be the point at which plastic instability is noted (fracture occurs shortly thereafter). In all tests, the instability is initiated in the localized region neighboring the hole. The monotonic test results are summarized in Table I.

CONSTANT AMPLITUDE

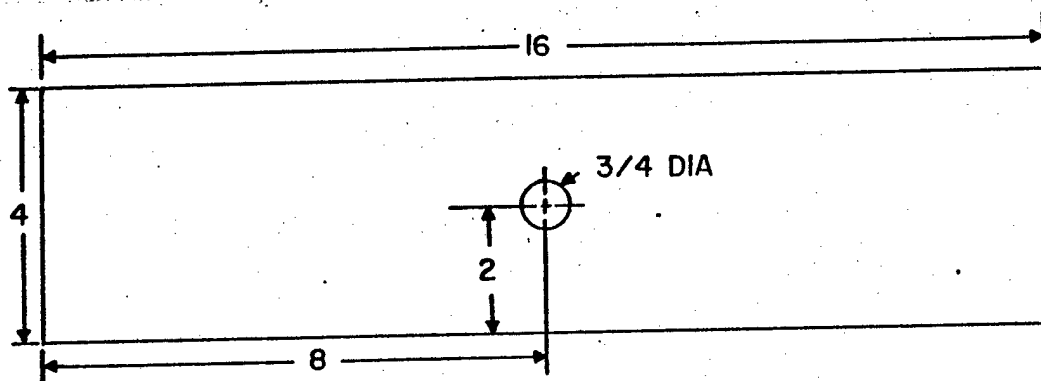
During the next set of tests, the load was cycled from zero to a maximum level that was a given percent of the average fracture stress in the monotonic tests. A sample constant amplitude load history applied to the Fig. 1 geometry is shown in Fig 3. The corresponding load vs crosshead displacement diagram is shown in Fig. 4. To establish the incremental specimen plastic displacement, the tensile permanent set between each cycle was determined from the load-displacement data, the resulting cumulative plastic displacement is illustrated in Fig. 5. The average plastic displacement for each constant amplitude test was calculated using the tensile plastic displacement increments associated with all applied load cycles prior to failure. Failure was defined as the first visual indication of crack initiation. As shown in Fig. 5, material hardening is exhibited for the first few cycles, and thereafter an ever increasing amount of softening occurs. This type of hardening-softening pattern was exhibited in all of the constant amplitude tests. The test data from the constant amplitude tests are given in Table 2.

TABLE I - DATA FROM MONOTONIC TESTS

| TEST NUMBER | TOTAL PLASTIC DISPLACEMENT | MAXIMUM LOAD AT FRACTURE | GROSS FRACTURE STRESS | NET FRACTURE STRESS |
|----------------|-------------------------------|--------------------------------|-----------------------------|---------------------------|
| | δ_{pl}^{cr} (inch) | P_{max} (kip) | σ_g (ksi) | σ_n (ksi) |
| 1 | 0.192 | 48.1 | 32.1 | 39.5 |
| 2 | 0.200 | 48.9 | 32.6 | 40.1 |
| 3 | 0.205 | 47.8 | 31.9 | 39.2 |
| 4 | 0.217 | 47.8 | 31.9 | 39.3 |
| Average | 0.204 | 48.2 | 32.1 | 39.5 |

TABLE II - DATA FROM CONSTANT AMPLITUDE TESTS

| TEST NUMBER | TEST CONDITION | TOTAL PLASTIC DISPLACEMENT | PERCENT OF MONOTONIC FRACTURE LOAD | δ_{pl}^{cr} (in) | CYCLES TO FAILURE | AVERAGE PER CYCLE PLASTIC DISPLACEMENT | MAXIMUM LOAD AT FAILURE | GROSS STRESS |
|----------------|-------------------|-------------------------------|---|----------------------------|----------------------|--|----------------------------|---------------------|
| | | | | | N_f | $\Delta\delta_{pl}$ (in) | P_{max} (kips) | σ_g (ksi) |
| 5 | 98 | 0.239 | | | 3 | 0.080 | 46.9 | 31.3 |
| 6 | 97 | 0.263 | | | 5 | 0.053 | 46.6 | 31.0 |
| 7 | 98 | 0.271 | | | 27 | 0.010 | 46.8 | 31.2 |
| 8 | 95 | 0.264 | | | 24 | 0.011 | 45.6 | 30.4 |
| 9 | 94 | 0.291 | | | 28 | 0.0104 | 45.4 | 30.2 |
| 10 | 93 | 0.227 | | | 32 | 0.0071 | 44.6 | 29.7 |
| 11 | 95 | 0.260 | | | 82 | 0.0032 | 45.9 | 30.6 |



ALL DIMENSIONS IN INCHES
THICKNESS = 0.375"

Figure 1. Test Geometry For Initial Damage Accumulation Study.

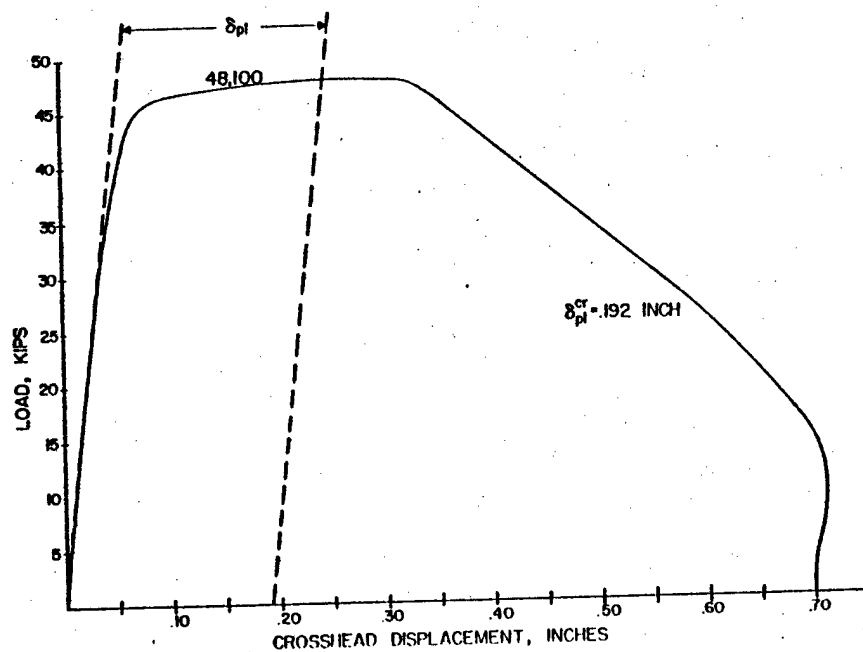


Figure 2. Monotonic Test Data.

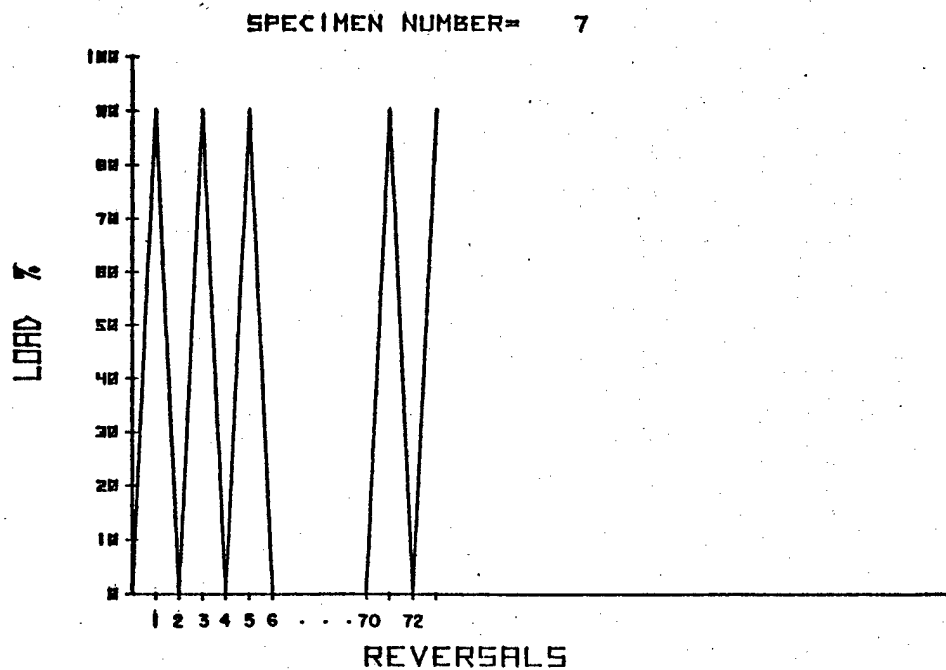


Figure 3. Programmed Constant Amplitude Loading For Test Number 10.

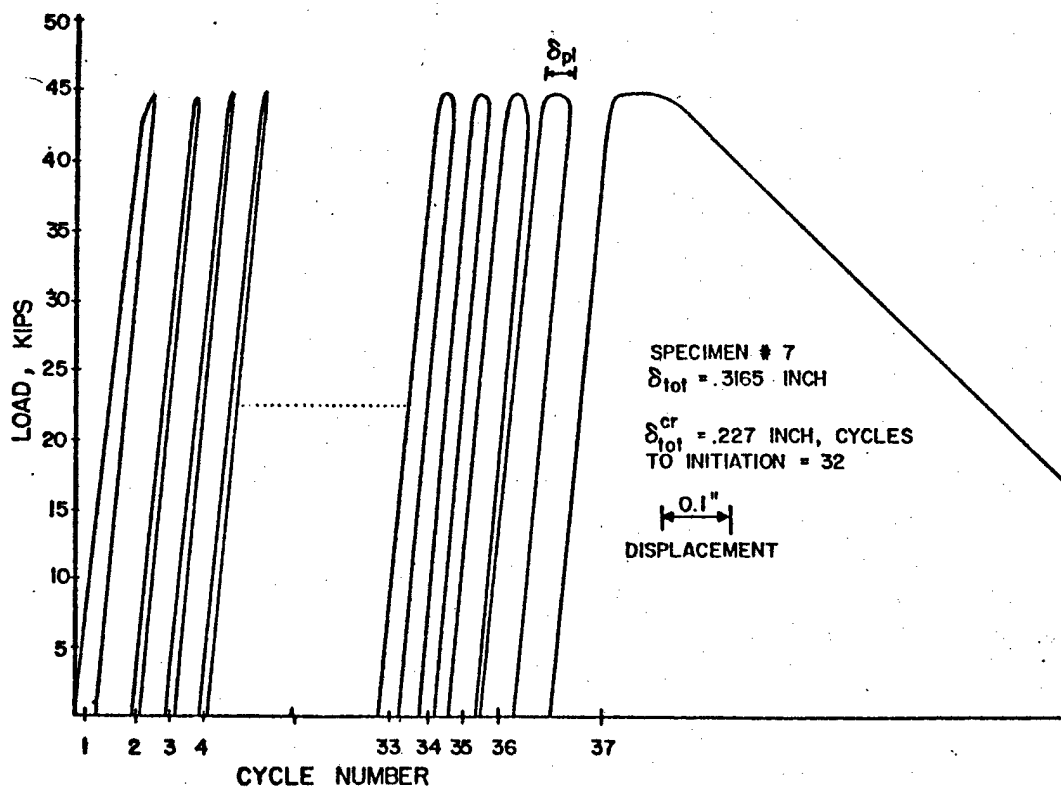


Figure 4. Constant Amplitude Test Data For Test Number 10.

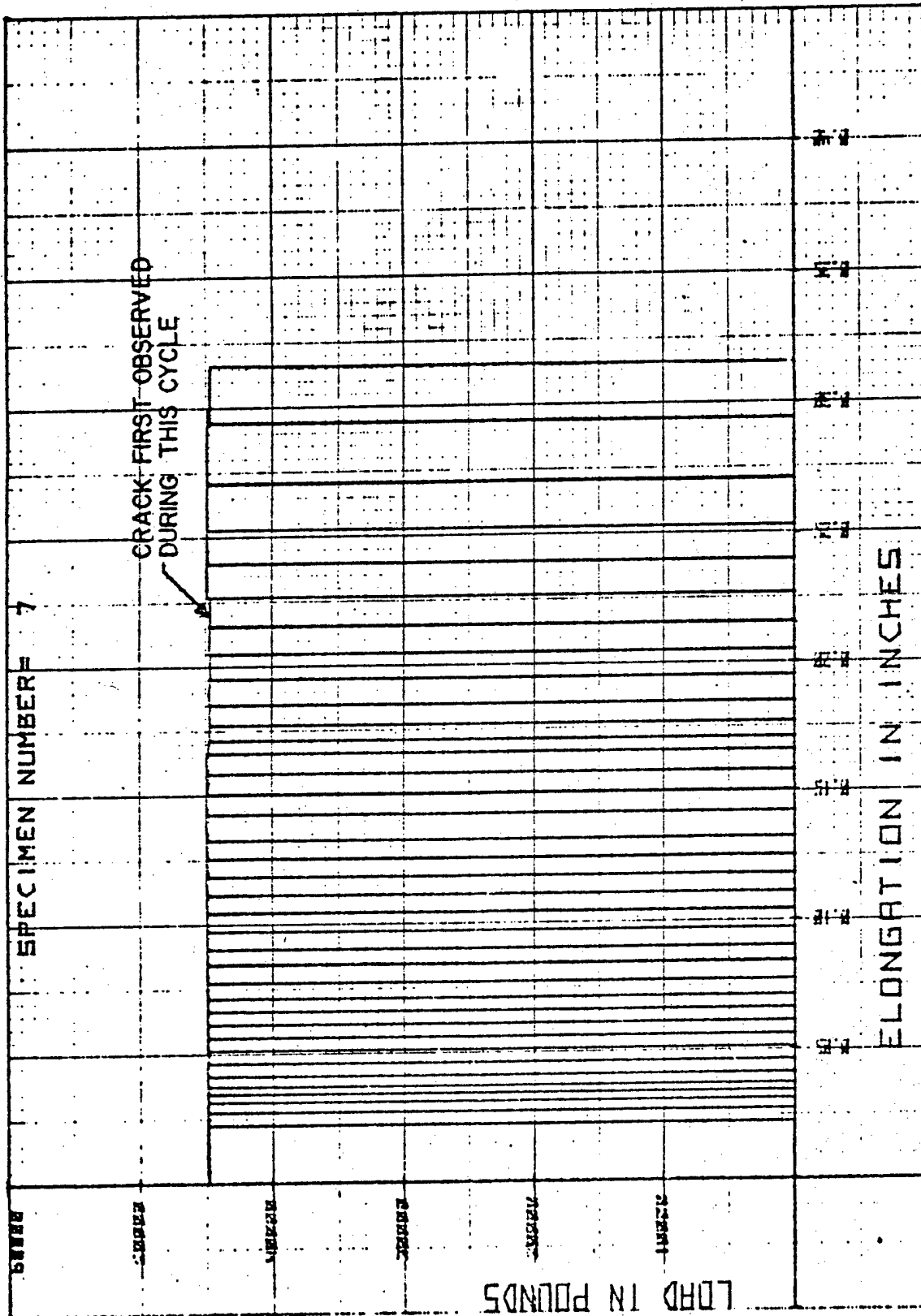


Figure 5. Plastic Crosshead Displacement Accumulation As A Function Of Constant Amplitude Cycles For Test Number 10.

DAMAGE ACCUMULATION METHODS

Method I utilizes an incremental plastic displacement-life method, which in equation form describes cycles to failure (N) as

$$N = C_1 \cdot \Delta\delta_{pl}^{n_1} \quad (1)$$

where C_1 and n_1 are experimentally determined constants. Damage per cycle (D) is calculated using the reciprocal of Eq. 1:

$$D = \frac{1}{C_1} \cdot \Delta\delta_{pl}^{-n_1} \quad (2)$$

The cycles to failure vs average plastic displacement per cycle were plotted for each test as shown in Fig. 6. A power law equation was fitted to these data in a least square manner to establish the constants C_1 and n_1 in Eq. 1. Figure 6 also provides the resulting equation where the determined values of C_1 and n_1 are 0.190 and 1.067, respectively.

Method II is based on a Neuber type parameter, which utilizes the product of the change in both plastic displacement and gross stress, i.e.

$$P = (\Delta\sigma_g \times \Delta\delta_{pl} \times E)^{1/2} \quad (3)$$

so that life estimates are made using

$$N = C_2 P^{n_2} \quad (4)$$

where C_2 and n_2 are experimentally determined constants. The damage per cycle (D) is obtained from the reciprocal of Eq. 4; therefore,

$$D = \frac{1}{C_2} P^{-n_2} \quad (5)$$

To determine the constants for Eq. 4, the Neuber parameter is calculated for the same data previously plotted in Fig. 6. The resulting power law least square equation and data are shown in Fig. 7. It can be seen that the constants $C_2 = 0.102 \times 10^6$ and $n_2 = 1.988$ adequately describe the data.

Upon further examination of the data in Tables I and II, it was noted that the monotonic plastic displacement at failure and the sum of the constant amplitude plastic displacement increments were similar. A third damage accumulation method (Method III) was formulated on the basis of this observation; thus the increment of damage per cycle (D) might be expressed as

$$D = \frac{\Delta\delta_{pl}}{\delta_{pl}^{cr}} \quad (6)$$

where $\Delta\delta_{pl}$ is the tensile plastic displacement per load cycle and δ_{pl}^{cr} is the average monotonic plastic displacement based on four tests ($\delta_{pl}^{cr} = 0.204$ in.). This method of calculating damage follows an exhaustion of ductility scheme (5).

Equation 6 was applied to obtain estimates of the damage increment per cycle which could then be summed for each applied load cycle to obtain a total damage estimate.

Since this ductility method depends solely on the monotonic displacement, it does not account for any cyclic variations that were observed during the constant amplitude tests.

VERIFYING THE APPLICABILITY OF THE DAMAGE METHODS

Damage estimates are now verified for the monotonic and constant-load amplitude tests using the experimentally measured (on a per cycle basis) load-plastic displacement data. Recall that average responses were used to generate the data given in Figs. 6 and 7. For Method I, (DISPLACEMENT METHOD), the per cycle tensile plastic displacement range is entered into Eq. 2 to calculate damage for this cycle. The total (accumulated) damage is achieved by summing all of the individual damages for each cycle. Method II (NEUBER METHOD) follows the same procedure except that the per cycle values of the Neuber parameter are calculated using Eq. 3 before substitution into Eq. 5, the Neuber parameter damage equation. For Method III (DUCTILITY METHOD) the damage estimate is achieved by summing the damage contributions of the individual per cycle tensile plastic displacement increments utilizing Eq. 6. The resulting damage summations are given in Table III for all tests introduced thus far.

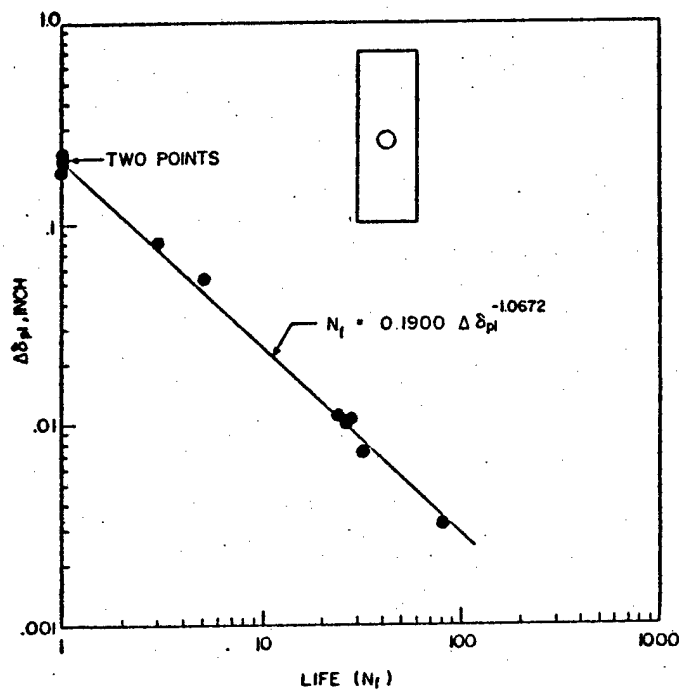


Figure 6. Plastic Crosshead Displacement Versus Cycles To Initiate A Crack, Based On Average Plastic Crosshead Displacement Values.

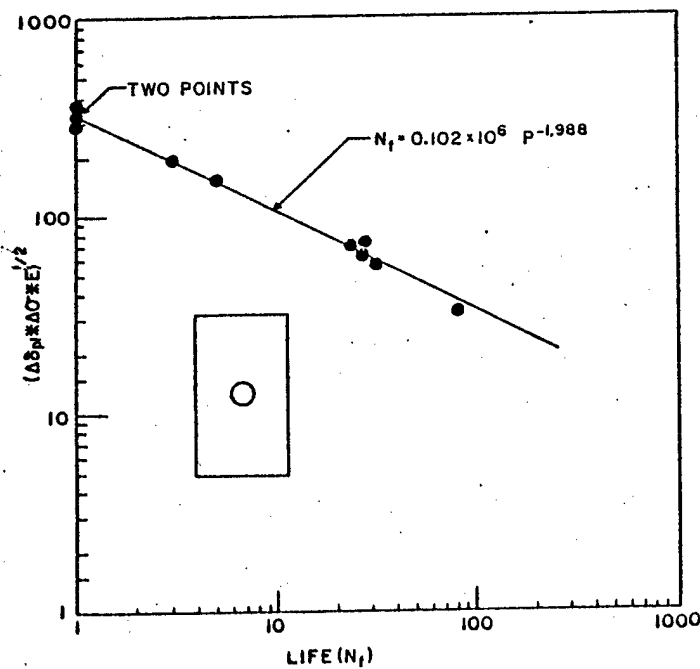


Figure 7. Neuber Parameter Versus Cycles To Initiate A Crack Based on Average Cyclic Values Of The Neuber Parameter.

TABLE III - DAMAGE SUMMATIONS BASED ON AVERAGE PER CYCLE
MEASUREMENTS ($\Sigma D > 1$, CONSERVATIVE)

| TEST NUMBER | DAMAGE METHOD | | | TYPE TEST |
|----------------|---------------|--------|-----------|--------------|
| | DISPLACEMENT | NEUBER | DUCTILITY | |
| 1 | 0.90 | 0.90 | 0.94 | MONOTONIC |
| 2 | 0.94 | 0.95 | 0.98 | " |
| 3 | 0.97 | 0.96 | 1.00 | " |
| 4 | 1.03 | 1.01 | 1.06 | " |
| 5 | 1.07 | 1.10 | 1.17 | CYCLIC |
| 6 | 1.15 | 1.21 | 1.29 | " |
| 7 | 1.07 | 1.26 | 1.33 | " |
| 8 | 1.04 | 1.20 | 1.30 | " |
| 9 | 1.15 | 1.33 | 1.43 | " |
| 10 | 0.86 | 1.01 | 1.11 | " |
| 11 | 0.97 | 1.20 | 1.27 | " |
| AVERAGE | 1.01 | 1.10 | 1.17 | |

SECTION III

NON-CONSTANT AMPLITUDE TESTING

PRELIMINARY TESTS - CORRELATION

To investigate the feasibility of applying damage methods to fatigue damage calculations for elements ahead of an advancing crack tip, an initial set of four stepwise increasing fatigue load tests were conducted on the notched specimens (Fig. 1 geometry). The stepwise loading history, the experimentally observed load-crosshead displacement, and derived load-plastic displacement for test number 12 are shown in Figs. 8, 9, and 10, respectively. The pertinent data for the complete set of four tests are presented in Table IV. As can be noted from Table IV, the stepwise increasing load increments varied between 1 and 5 percent (per cycle) of the monotonic fracture load. The selection of the stepwise increment and the initial starting load level for each successive test was based on a desire to refine our understanding of the data obtained in the previous tests.

The tests described above can be used to determine if the previously established constants for Eqs. 1, 4, and 6 are applicable to non-constant amplitude types of loading. All three damage methods were used to analyze the data from these tests; and, the damage estimates are summarized in Table V. All three damage methods are conservative in that they predict failure before the specimens actually failed (damages are greater than one at failure). The increasing load-amplitude damages associated with these tests agreed quite well with the constant load-amplitude damages, even though the local stress history at the notch and

TABLE IV - RESULTS FOR INITIAL STEPWISE INCREASING LOAD TESTS

| TEST NUMBER | TEST CONDITION | LOAD INCREMENT | TOTAL PLASTIC DIS- PLACEMENT | CYCLES TO FAILURE | MAXIMUM LOAD AT FAILURE | GROSS STRESS AT FAILURE |
|----------------|--|--|---------------------------------------|-------------------------|--------------------------------|-------------------------------|
| | Percent of Monotonic Fracture Load | Percent of Monotonic Fracture Load | δ_{pl} (in) | N | P _{max} (kips) | σ_g (ksi) |
| 12 | 0-50, 0-52 0-54, ... | 2 | 0.252 | 24 | 47.2 | 31.4 |
| 13 | 0-50, 0-55 0-60, ... | 5 | 0.248 | 11 | 47.7 | 31.8 |
| 14 | 0-80, 0-85 0-90, ... | 5 | 0.249 | 5 | 47.5 | 31.6 |
| 15 | 0-91, 0-92 0-93, ... | 1 | 0.265 | 7 | 46.3 | 30.8 |

TABLE V - DAMAGE METHODS COMPARED FOR INITIAL
STEPWISE INCREASING LOAD TESTS

| TEST NUMBER | DAMAGE METHOD | | |
|----------------|---------------|--------|-----------|
| | DISPLACEMENT | NEUBER | DUCTILITY |
| 12 | 1.08 | 1.12 | 1.24 |
| 13 | 1.10 | 1.12 | 1.21 |
| 14 | 1.11 | 1.14 | 1.22 |
| 15 | 1.13 | 1.21 | 1.30 |
| AVERAGE | 1.10 | 1.15 | 1.24 |

plastic deformation patterns per cycle were substantially different. The reason for this closeness in behavior depends primarily on the last few load cycles where the plastic displacement, as well as the damage per cycle becomes incrementally larger. This point is illustrated graphically in Fig. 11 where the damage accumulation calculation for test number 12 is described as a function of the maximum stress level in a load cycle. Recall that test number 12 was first loaded to the fifty (50) percent level and the stepwise increment was two (2) percent of the monotonic ultimate strength. The first ninety (90) percent of the load cycles in this test resulted in an accumulated damage less than 0.2; this observation is independent of the method of damage calculation.

A TEST OF THE DAMAGE CALCULATION

To challenge the validity of the three methods, damages were to be predicted for a second set of stepwise increasing load-amplitude tests. If the life, the reciprocal of damage, could be accurately predicted then the validity of a damage method would be established.

For all three methods, the plastic displacement must be known, since, it is used to calculate a damage estimate using Eqs. 2, 5, and 6. For the previous damage calculations, the measured (per cycle) plastic displacements were used; for the predictive mode, however, an alternate estimate of displacement must be utilized. Data from Tests 12 through 15 were utilized to form the relationship between load and accumulated plastic displacement that is shown in Fig. 12. The analytical equivalent to the curve shown in Fig. 12 is

$$\sigma_g = \begin{cases} 61.526(\Sigma\Delta\delta_{p1})^{0.22314} & \text{when } \sigma_g \leq 30.21\text{ksi,} \\ 32.354(\Sigma\Delta\delta_{p1})^{0.021543} & \text{when } \sigma_g > 30.21\text{ksi} \end{cases} \quad (7)$$

Equation 7 is used to determine the accumulated displacement for the maximum stress in each applied load cycle. The difference between the accumulated displacement between two successive stepwise increasing load cycles represents the estimate of the plastic displacement for the current load cycle. This estimate is substituted into the various damage relationships to determine the damage occurring during that cycle. The estimating process is repeated until the damage sums to 1.0, the level associated with failure. The prediction capability of this scheme was first tested for those load histories employed in tests 12 through 15. The life predictions are shown in Table VI. As expected, the results closely follow the actual test lives, since the basic load versus plastic displacement data were derived from these tests.

TABLE VI - VERIFICATION LIFE ESTIMATES (CYCLES TO FAILURE)
BASED ON THE THREE DAMAGE METHODS

| TEST NUMBER | PREDICTED LIFE | | | OBSERVED LIFE |
|----------------|----------------|--------|-----------|------------------|
| | DISPLACEMENT | NEUBER | DUCTILITY | |
| 12 | 25 | 25 | 25 | 24 |
| 13 | 11 | 11 | 11 | 11 |
| 14 | 5 | 5 | 5 | 5 |
| 15 | 9 | 9 | 8 | 7 |

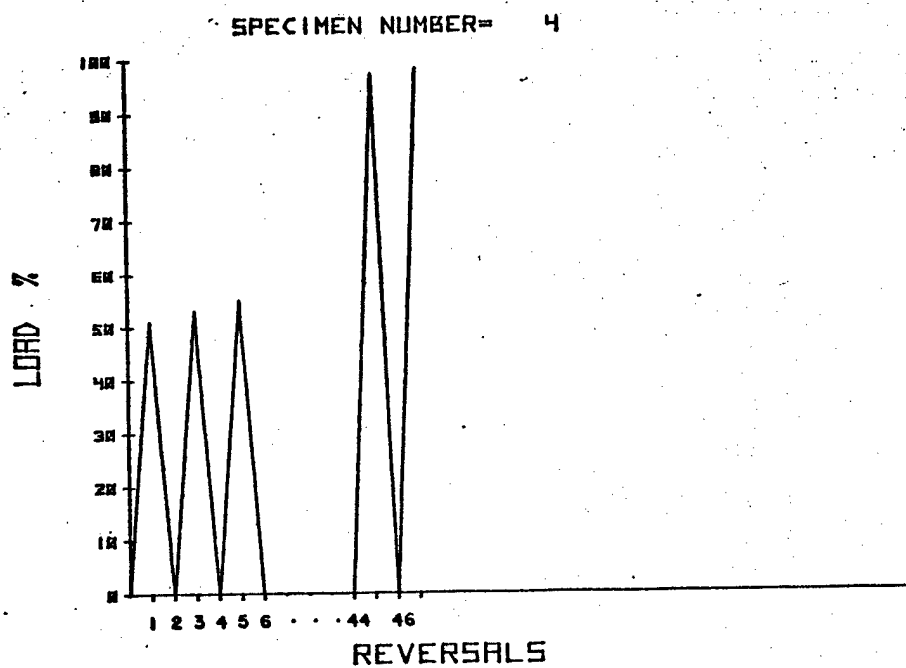


Figure 8. Programmed Stepwise Increasing Amplitude Loading For Test Number 12.

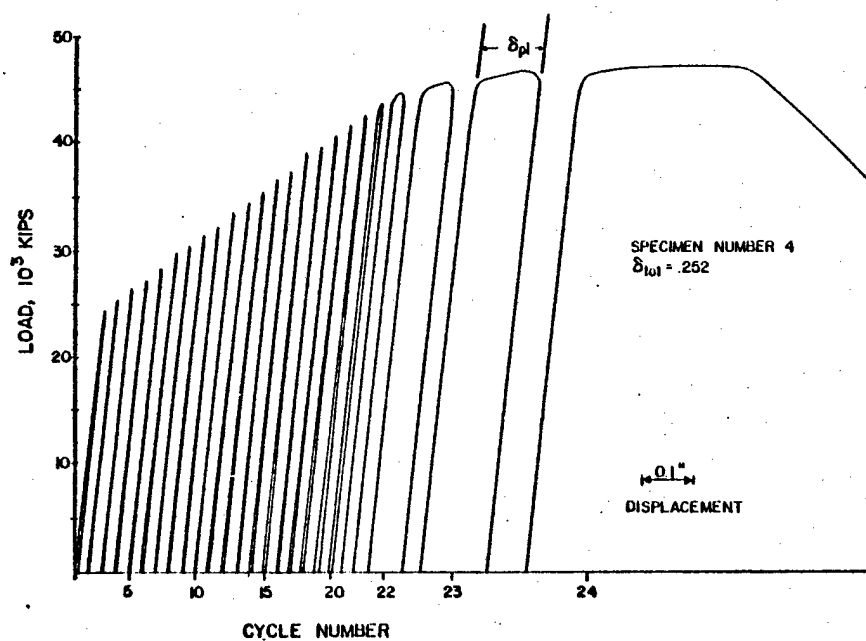


Figure 9. Stepwise Increasing Amplitude Test Data For Test Number 12.

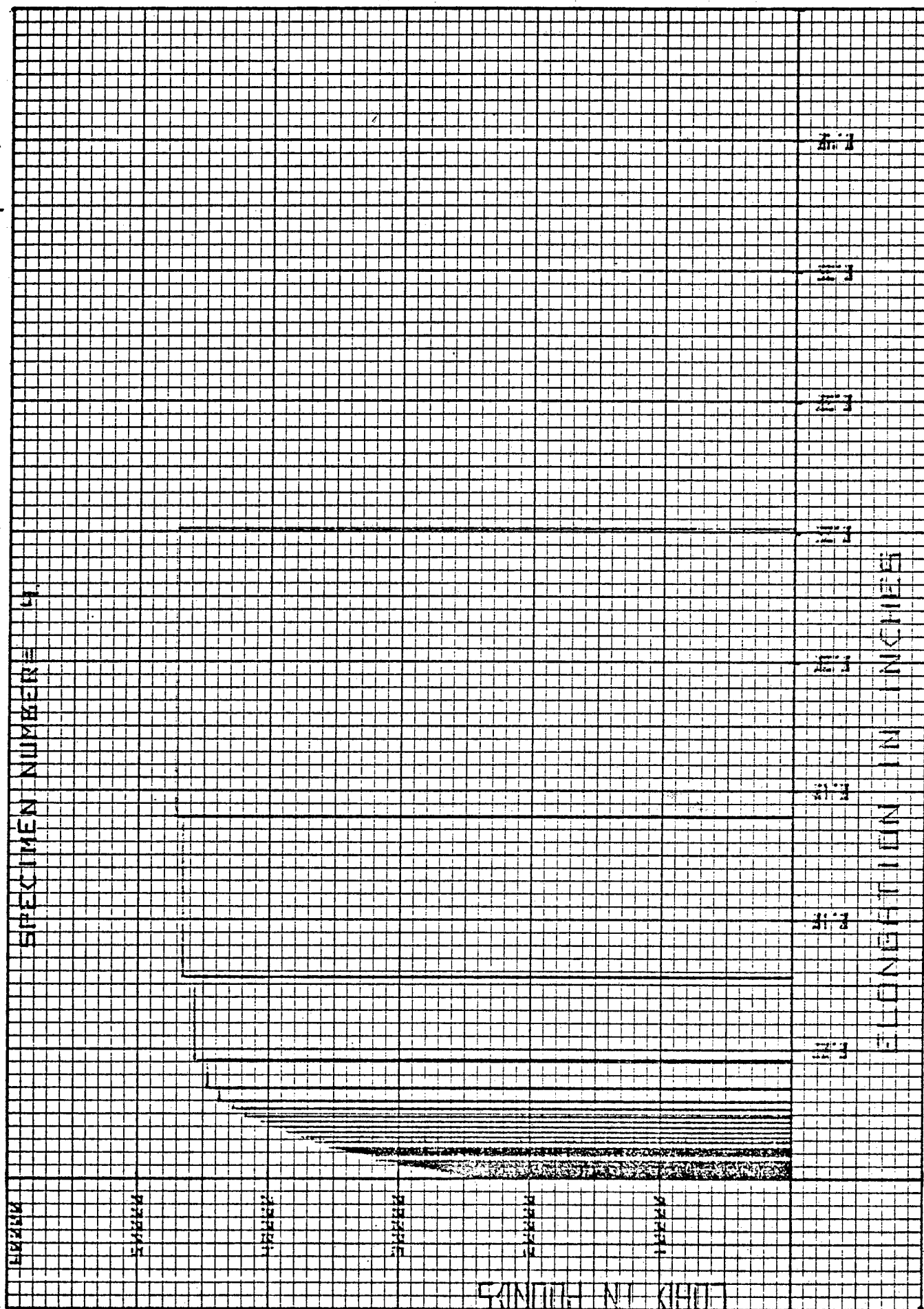


Figure 10. Plastic Crosshead Displacement As A Function of Cycles For Test Number 12.

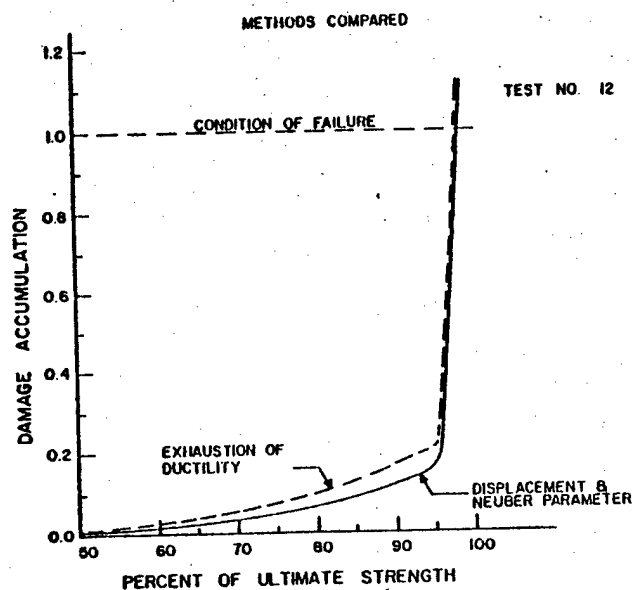


Figure 11. Damage Accumulation As A Function Of Stress Level For Test Number 12.

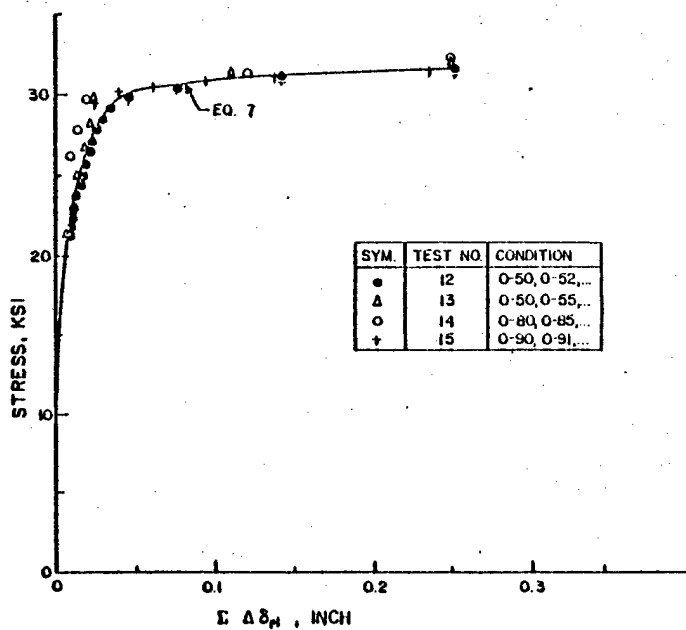


Figure 12. Test Specimen Gross Stress As A Function Of Accumulated Plastic Crosshead Displacement.

ESTIMATING LIFE BEHAVIOR IN ADVANCE

A second set of stepwise increasing load-amplitude tests were contemplated and the predictive scheme was applied in advance to determine an estimate of cycles to failure. Table VII summarizes the cyclic test conditions contemplated for the new set of four tests. The resulting life predictions (cycles to failure) are presented and compared to the observed failure behavior in Table VIII. Table IX summarizes the other pertinent test data.

As can be noted from Table VIII, the predicted lives were conservative for Tests 16, 17, and 19 and slightly unconservative for Test 18. While the errors in the life prediction calculations were larger than that observed in the previous test set when the plastic displacement per cycle was known, we believe that the estimates are sufficiently close to offer additional encouragement for calculations that follow schemes similar to that described here.

The damage estimates that result from using the incremental (tensile) plastic displacements observed in Tests 16 through 19 in Eqs. 2, 5, and 6 are given in Table X. The Neuber Method appears to exhibit the largest variability in damage estimates. While there does not appear to be any reason for the low damage estimate for Test 16 using the Neuber Method, the estimates for Tests 18 and 19 might have been better if a damage scheme based on the maximum stress rather than the stress range had been used. Tests 18 and 19 differ from the other constant amplitude and stepwise-increasing load tests in that the minimum load is controlled at a level other than zero.

TABLE VII - CONDITIONS FOR A NEW SET OF STEPWISE
INCREASING FATIGUE LOAD TESTS

| TEST NUMBER | MIN-MAX CYCLE CONDITION | INCREMENTAL INCREASE IN MAXIMUM LOAD |
|----------------|---|---|
| | Percent of Monotonic Fracture Load | Percent of Monotonic Fracture Load |
| 16 | 0-90, 0-91, 0-92, 0-93, 0-94, ... | 1 |
| 17 | 0-90, 0-91, 0-92, 0-94, 0-96, ... | 1 then 2 |
| 18 | 0-90, +50-92, +50-94, ... | 2 |
| 19 | -50-80, -50-82, -50-84, -50-86, -50-88, ... | 2 |

TABLE VIII - LIFE ESTIMATES (CYCLES TO FAILURE) FOR A NEW
SET OF STEPWISE INCREASING FATIGUE LOAD TESTS

| TEST NUMBER | PREDICTED LIFE | | | OBSERVED LIFE |
|----------------|----------------|--------|-----------|------------------|
| | DISPLACEMENT | NEUBER | DUCTILITY | |
| 16 | 9 | 9 | 9 | 12 |
| 17 | 6 | 6 | 6 | 6 |
| 18 | 5 | 6 | 5 | 3 |
| 19 | 10 | 10 | 10 | 9 |

TABLE IX - FAILURE DATA FOR SECOND SET OF
STEPWISE-INCREASING LOAD TESTS

| TEST NUMBER | TOTAL PLASTIC DISPLACEMENT AT FAILURE | CYCLES TO FAILURE | MAXIMUM LOAD AT FAILURE | GROSS STRESS AT FAILURE |
|----------------|---|----------------------|-------------------------------|-------------------------------|
| | δ_{pl} (inch) | N_f | P_{max} (kips) | σ_g (ksi) |
| 16 | 0.210 | 12 | 48.9 | 32.6 |
| 17 | 0.210 | 6 | 47.7 | 31.8 |
| 18 | 0.264 | 3 | 47.4 | 31.6 |
| 19 | 0.240 | 9 | 45.7 | 30.5 |

TABLE X - DAMAGE CALCULATIONS FOR STEP-WISE INCREASING
LOAD TESTS DESCRIBED BY TABLE IX; BASED ON
PLASTIC DISPLACEMENT TEST RESULTS

| TEST NUMBER | DAMAGE METHOD | | |
|----------------|---------------|--------|-----------|
| | DISPLACEMENT | NEUBER | DUCTILITY |
| 16 | 0.88 | 0.66 | 1.03 |
| 17 | 0.90 | 0.98 | 1.03 |
| 18 | 1.19 | 0.87 | 1.29 |
| 19 | 1.05 | 1.61 | 1.18 |

DATA-ANALYSIS SUMMARY

Table XI summarizes the damage estimates individually presented in Tables III, V and X. The plastic-displacement method can be seen to provide the best estimates of impending failure (its average is closest to 1.0 and its standard deviation is closest to 0). Of the three methods, the plastic-displacement method also has the smallest maximum error in anticipating the experimentally expected result (1.0); this deviation is +19% for the plastic-displacement method, +61% for the Neuber method and +43% for the Exhaustion of Ductility Method. It might be noted that the Exhaustion of Ductility Method gives conservative estimates of damage for all the cyclic tests (Recall that Tests 1 and 2 are monotonic load tests).

Based on the success achieved in applying the simplified damage accumulation relationships (discussed herein) for predicting the fatigue initiation behavior of notched coupons subjected to stepwise-increasing loads, it is recommended that additional work be conducted to explore the following: (a) notch acuity (See Appendix A), (b) relationship between crosshead plastic displacement and notch root stress and strain fields, and (c) mechanical factors that can be related to the fatigue damage accumulation process in high gradient stress strain fields.

TABLE XI - DAMAGE CALCULATIONS SUMMARIZED FOR ALL TESTS

| TEST NUMBER | DAMAGE METHOD | | |
|----------------|---------------|--------|-----------|
| | DISPLACEMENT | NEUBER | DUCTILITY |
| 1 | 0.90 | 0.90 | 0.94 |
| 2 | 0.94 | 0.95 | 0.98 |
| 3 | 0.97 | 0.96 | 1.00 |
| 4 | 1.03 | 1.01 | 1.06 |
| 5 | 1.07 | 1.10 | 1.17 |
| 6 | 1.15 | 1.21 | 1.29 |
| 7 | 1.07 | 1.26 | 1.33 |
| 8 | 1.04 | 1.20 | 1.30 |
| 9 | 1.15 | 1.33 | 1.43* |
| 10 | 0.86 | 1.01 | 1.11 |
| 11 | 0.97 | 1.20 | 1.27 |
| 12 | 1.08 | 1.12 | 1.24 |
| 13 | 1.10 | 1.12 | 1.22 |
| 14 | 1.11 | 1.14 | 1.22 |
| 15 | 1.13 | 1.21 | 1.30 |
| 16 | 0.88 | 0.66 | 1.03 |
| 17 | 0.90 | 0.98 | 1.03 |
| 18 | 1.19* | 0.87 | 1.29 |
| 19 | 1.05 | 1.61* | 1.18 |
| AVERAGE | 1.03 | 1.10 | 1.18 |
| STD. DEV. | 0.10 | 0.20 | 0.14 |

*Represents largest deviation from experimentally observed result (1.0) for the given method.

SECTION IV

CONCLUSIONS

Based on this limited feasibility study, the following conclusions appear evident:

1. The damage accumulation process (DAP) associated with initiating fatigue cracks in notched coupons subjected to stepwise increasing amplitude loading histories can be described using a constant amplitude data base and a knowledge of cyclic plastic deformation occurring in the coupon.
2. The basic hypothesis normally utilized in calculating the rate of crack movement based on low cycle fatigue methodologies appears reasonable. Unfortunately, no attempt was made to relate unnotched coupon behavior established by constant amplitude loading to the notched coupon behavior exhibited during stepwise increasing amplitude loadings.

SECTION V

REFERENCES

1. Fleck, W. G., and Anderson, R. B., "A Model Study of the Characteristics of Fatigue Crack Extension," Proceedings of the Air Force Conference on Fatigue and Fracture of Aircraft Structures and Materials, edited by H. A. Wood et. al., AFFDL-TR-70-144, Air Force Flight Dynamics Laboratory, Wright-Patterson AFB, OH, Sept 1970.
2. Lehr, K. and Liu, H. W., "Fatigue Crack Propagation and Strain Cycling Properties," International Journal of Fracture Mechanics, Vol. 5, No. 1, pp. 45-55 (1969).
3. Majumdar, S. and Morrow, J., "Correlation between Fatigue Crack Propagation and Low Cycle Fatigue Properties," Fracture Toughness and Slow-Stable Cracking, ASTM STP 559, American Society for Testing and Materials, pp. 159-182 (1974).
4. Mowbray, D. F., "Derivation of a Low-Cycle Fatigue Relationship Employing the J-Integral Approach to Crack Growth," Cracks and Fracture, ASTM STP 601, American Society for Testing and Materials, pp. 33-46 (1976).
5. Sandor, B. I., Fundamentals of Cyclic Stress and Strain, The University of Wisconsin Press, Madison, Wisconsin, 1972.

APPENDIX A

To investigate the effect that a different notch geometry has on the damage accumulation process, an additional set of tests were performed on copper coupons which contained a slot (1/8 inch high by 3/4 inch wide) rather than the 3/4 inch diameter hole (Fig. 1 geometry). The data resulting for the monotonic and constant amplitude tests are given in Table A1. Following the procedures established in the text, new constants were developed for the damage accumulation equations (Eqs. 2, 5, and 6). Again, the average cyclic plastic displacement was calculated by dividing the total plastic displacement by the number of cycles.

Figure A1 compares the plastic displacement-life data with Eq. A1 and with the Equation shown in Fig. 6 for the (round) hole data. Equation A1 was established in a least-squares manner using the data shown in Fig. A1:

$$N_f = 0.113 \Delta\delta_{pl}^{-1.1278} \quad (A1)$$

As shown by Fig. A1, the equation for the slot data has a slope that is similar to that of the hole data. Also, one can note that the slot with its increased notch acuity represents a more damaging condition when the controlling parameter is assumed to be (crosshead) plastic displacement.

Figure A2 compares the Neuber Parameter-Life data with Eq. A2 and the (round) hole equation presented in Fig. 7. Equation A2 was established in a least-squares manner using the data presented in Fig. A2:

$$N_f = 0.996 \times 10^5 (P)^{-2.050} \quad (A2)$$

Again the slot equation has about the same slope and indicates a more damaging condition when compared to the hole equation.

Based on Table A1, the Exhaustion of Ductility Method would utilize the monotonic load test plastic displacement value of failure (= 0.147 inch) in its calculation scheme.

A single stepwise-increasing load amplitude test was conducted for the slot notch geometry. The initial stepwise-increasing maximum load level was set at 90 percent of the monotonic fracture level and the step increment was 2 percent. The damages calculated for all the slot notch tests (monotonic, constant amplitude, and stepwise-increasing) using each of the three damage methods are given in Table A2. Again, the plastic displacement method appears to provide the best estimate of impending failure when based on the experimentally observed (per cycle) plastic displacement levels.

The similarity of the results observed for the slot notched coupons and the hole notched coupons suggests that the cyclic plastic displacement plays a controlling role in developing crack movement in local regions that are experiencing more intense plastic straining conditions. The next step in the process of increasing our understanding of this process will be to relate the crosshead plastic displacement to the more intense plastic strain conditions at the crack initiation site.

TABLE A1 - SUMMARY OF TEST DATA FOR SLOTTED TEST SPECIMENS

| Test Number | Condition | Total Plastic Displacement | Cycles To Failure | Average Plastic Displacement Based on All Cycles | Maximum Load At Failure | Gross Stress |
|-------------|------------------------|----------------------------|-------------------|--|-------------------------|---------------------|
| | | δ_{pl} (inch) | N_f | $\Delta\delta_{pl}$ (inch) | P_{max} (kip) | σ_g (ksi) |
| 20 | Monotonic to fail | 0.147 | 1 | 0.147 | 48.0 | 32.0 |
| 21 | Monotonic to fail | 0.147 | 1 | 0.147 | 47.9 | 31.9 |
| 22 | 90% Constant Amplitude | 0.180 | 12 | 0.015 | 44.6 | 29.7 |
| 23 | 90% Constant Amplitude | 0.228 | 53 | 0.004 | 44.8 | 29.9 |
| 24 | 85% Constant Amplitude | 0.277 | 281 | 0.001 | 42.3 | 28.2 |

TABLE A2 - DAMAGE CALCULATIONS SUMMARIZED FOR SLOTTED SPECIMENS

| Test Number | Condition | Damage Method | | |
|----------------|--------------------------------------|---------------|--------|-----------|
| | | Displacement | Neuber | Ductility |
| 20 | Monotonic | 1.02 | 1.00 | 1.00 |
| 21 | " | 1.02 | 1.00 | 1.00 |
| 22 | Constant Amplitude | 0.98 | 1.09 | 1.22 |
| 23 | " | 1.04 | 1.33 | 1.55 |
| 24 | " | 1.10 | 1.48 | 1.88 |
| 25 | Stepwise- Increasing Amplitude | 0.90 | 0.97 | 1.05 |
| Average | | 1.01 | 1.14 | 1.28 |

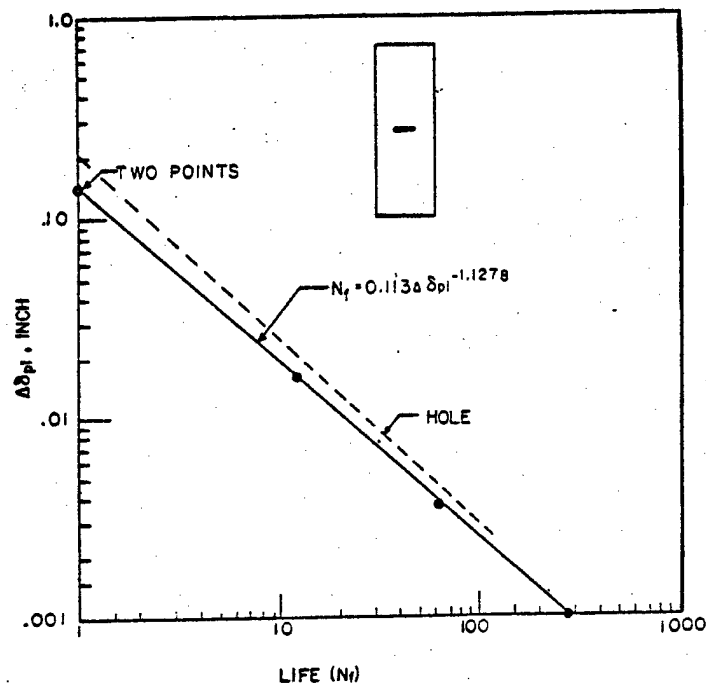


Figure A1. Plastic Crosshead Displacement Vs. Cycles To Failure For Slot Geometry.

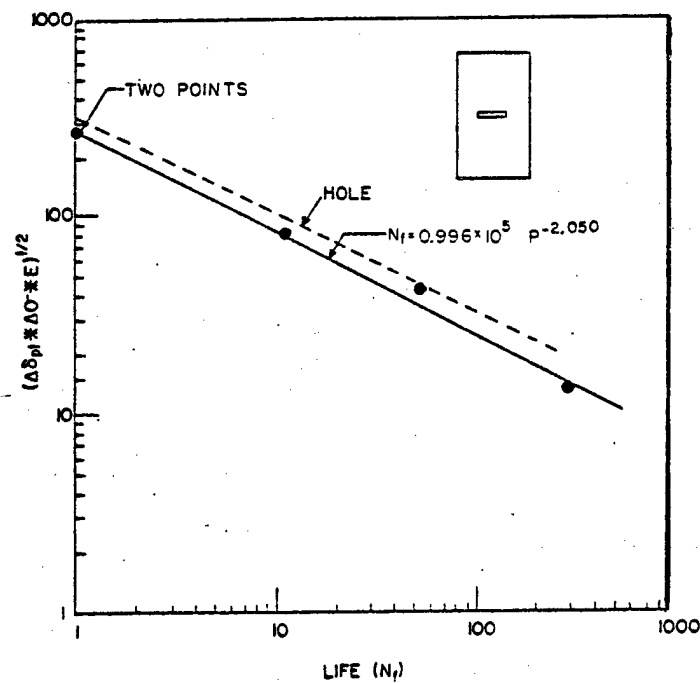


Figure A2. Neuber Parametric Vs. Cycles To Failure For Slot Geometry.